

# $\beta/\gamma$ Oscillatory Activity in the CA3 Hippocampal Area Is Depressed by Aberrant GABAergic Transmission from the Dentate Gyrus after Seizures

Mario Treviño, Carmen Vivar, and Rafael Gutiérrez

Departamento de Fisiología, Biofísica y Neurociencias, Centro de Investigación y de Estudios Avanzados, México DF 07000, México

Oscillatory activity in the CA3 region is thought to be involved in the encoding and retrieval of information. These oscillations originate from the recurrent excitation between pyramidal cells that are entrained by the synchronous rhythmic inhibition of local interneurons. We show here that, after seizures, the dentate gyrus (DG) tonically inhibits  $\beta/\gamma$  (20–24 Hz) field oscillations in the CA3 area through GABA-mediated signaling. These oscillations originate in the interneuron network because they are maintained in the presence of ionotropic glutamate receptor antagonists, and they can be blocked by GABA<sub>A</sub> receptor antagonists or by perfusion of a calcium-free extracellular medium. Inhibition of this oscillatory activity requires intact DG-to-CA3 connections, and it is suppressed by the activation of metabotropic glutamate receptors (mGluR). The influence of mGluR activation was reflected in the spontaneous subthreshold membrane oscillations of CA3 interneurons after one seizure but could also be observed in pyramidal cells after several seizures. Coincident stimulation of the DG at  $\theta$  and  $\beta/\gamma$  frequencies produced a frequency-dependent excitation of interneurons and the inhibition of pyramidal cells. Indeed, these effects were maximal at the frequency that matched the mGluR-sensitive spontaneous field oscillations, suggesting a resonance phenomenon. Our results shed light on the mechanisms that may underlie the deficits in memory and cognition observed after epileptic seizures.

**Key words:** mossy fibers; plasticity; GABA; CA3; mGluR; oscillations

## Introduction

$\beta/\gamma$  oscillations (20–80 Hz) can be observed in several cortical regions, including the hippocampal formation in which they are thought to assist in the encoding and retrieval of memory traces. These oscillations may be a representation of the information itself, or, alternatively, they may regulate the flow of information in the neural circuits (Sejnowski and Paulsen, 2006). Within these circuits, the pyramidal cells (PyrC) are thought to encode, process, store, and retrieve information, whereas the interneurons (Int) are believed to control the spike timing of principal neurons and the network oscillations (Buzsáki and Chrobak, 1995).

Information from the entorhinal cortex reaches the hippocampal CA3 area directly via the perforant pathway and indirectly by way of the mossy fibers (MF) of the granule cells. Moreover, the interneurons and not the PyrC are the major targets of the MF in the CA3 (Amaral et al., 1990; Acsády et al., 1998).

Although fast oscillations in the dentate gyrus (DG) are driven by extrahippocampal cortical inputs (Bragin et al., 1995), the CA3–CA1 system appears to form an intrinsic intrahippocampal  $\gamma$  generator, in which the oscillation is generated in the recurrent CA3 network before it then propagates to the CA1 (Csicsvari et al., 2003). However, PyrC are entrained by the synchronous rhythmic inhibition that originates from GABAergic interneurons (Wang and Buzsáki, 1996; Mann et al., 2005a,b).

There is compelling evidence of GABAergic transmission from the DG to the CA3 (for review, see Gutiérrez, 2005). This putative GABAergic signaling fulfills the physiological and pharmacological criteria of transmission of an MF origin, and it occurs under two circumstances: initially during early development (Walker et al., 2001; Gutiérrez et al., 2003; Kasyanov et al., 2004; Gómez-Lira et al., 2005; Safulina et al., 2006), and, subsequently, in the adult, it can be seen after seizures *in vivo* (Gutiérrez, 2000; Gutiérrez and Heinemann, 2001; Romo-Parra et al., 2003) or after repeated long-term potentiation-like stimulation *in vitro* (Gutiérrez, 2002). Because stimulation of the MF produces monosynaptic GABA<sub>A</sub> receptor (GABA<sub>A</sub>R)-mediated responses in both PyrC and interneurons of CA3, it seems reasonable to propose that the GABAergic transmission from the MF would influence the CA3 area as a whole (Treviño and Gutiérrez, 2005). Therefore, we hypothesized that the direct GABAergic inputs from the DG can modulate the intrinsic oscillatory activity of the CA3 after a single seizure and that the effect is more robust after inducing a permanent epileptic state by kindling.

Received Sept. 1, 2006; revised Nov. 29, 2006; accepted Dec. 1, 2006.

This work was supported by a grant from the Consejo Nacional de Ciencia y Tecnología (CONACYT) (R.G.). M.T. and C.V. were both supported by CONACYT, and they are students in the Neurosciences PhD program at the Universidad Nacional Autónoma de México and Centro de Investigación y de Estudios Avanzados, respectively. We thank Drs. Yoel Yaari, L. Menéndez de la Prida, and A. Draguhn for helpful discussions and Benjamín Muñoz and Beatriz Osorio for excellent technical assistance.

Correspondence should be addressed to Dr. Rafael Gutiérrez, Departamento de Fisiología, Biofísica y Neurociencias, Centro de Investigación y de Estudios Avanzados, Apartado Postal 14-740, México DF 07000, México. E-mail: grafael@fisio.cinvestav.mx.

DOI:10.1523/JNEUROSCI.3815-06.2007

Copyright © 2007 Society for Neuroscience 0270-6474/07/270251-09\$15.00/0

We found here that spontaneous  $\beta/\gamma$  field activity in the CA3 area of hippocampal slices from rats that have suffered seizures is strongly modulated by a GABAergic input from the DG. We could determine that the GABAergic input from the DG primarily affects the fundamental component of the CA3 oscillatory GABAergic system, the interneurons. Altogether, our results suggest that the direct modulation of  $\beta/\gamma$  oscillations in the CA3 by GABA from DG inputs can prevent the buildup of excitation and possibly hamper the storage of information in the hippocampal network after seizures.

## Materials and Methods

**Animals.** In these experiments, we used adult (230 g) Wistar rats distributed into three groups: (1) control group, (2) rats subjected to a single seizure, and (3) rats subjected to five to seven seizures. Whereas single seizures were produced by an intraperitoneal injection of pentylenetetrazol (PTZ) (60 mg/kg) (Gutiérrez, 2000), a model of seizures, repetitive seizures were produced by electrical kindling that produces a permanent epileptic state. *In vivo* kindled animals were surgically implanted with a stimulating electrode in the amygdala under ketamine anesthesia (60 mg/kg, i.p.). Subsequently, they were stimulated as described previously (Gutiérrez, 2000) until five to seven consecutive generalized tonic-clonic seizures had been induced. All experimental procedures were approved by the Ethical Committee on Animal Research at our institution.

**Slice preparation.** The rats were decapitated under deep ether anesthesia. The rats subjected to seizures were decapitated within 1 h after the seizure was provoked, and their brains were removed rapidly. Combined entorhinal cortex–hippocampus slices of 400  $\mu\text{m}$  were obtained with a vibraslicer (Campden Instruments, Lafayette, IN) submerged in oxygenated artificial CSF (ACSF) at 4°C, and they were kept in oxygenated ACSF at room temperature until they were used. The composition of the ACSF was as follows (in mM): 129 NaCl, 3 KCl, 1.25  $\text{NaH}_2\text{PO}_4$ , 1.8  $\text{MgSO}_4$ , 1.6 or 0  $\text{CaCl}_2$ , 20  $\text{NaHCO}_3$ , and 10 glucose, pH 7.35 (at 33°C). For experiments in which the MF pathway was disrupted, an incision was made through the CA3 area from the edge of the upper blade to the edge of the lower blade of the granular cell layer of the DG using a microknife. These slices were maintained in a recording chamber for at least 4 h after the cut was made before recording commenced.

**Recordings.** For extracellular and intracellular recordings, the slices were placed in a liquid-to-air interface recording chamber that was constantly perfused (1 ml/min) with ACSF at 32°C. Extracellular activity was recorded from the pyramidal cell layer of CA3b using borosilicate microelectrodes, pulled to yield 8–12 M $\Omega$  and filled with NaCl (155 mM). Intracellular activity was recorded from PyrC and interneurons located at the border of the pyramidal cell layer and stratum lucidum (SL) of CA3b with microelectrodes of 70–90 M $\Omega$  filled with potassium acetate (2 M) and biocytin (2%), the latter being used for *post hoc* anatomical identification of the cells. Extracellular and intracellular signals were recorded with Axoclamp 2B (Molecular Devices, Palo Alto, CA) amplifiers, and they were digitized (Digidata 1200; Molecular Devices) and acquired with the pClamp8 program (Molecular Devices) for off-line analysis. To evoke synaptic responses, stimulation at different frequencies (pulse duration, 0.1 ms) was applied over the molecular layer of the DG with bipolar glass-insulated platinum wire electrodes (25  $\mu\text{m}$ ).

**Data analysis.** The synaptic responses of PyrC and SL-Int to DG stimulation were recorded with sharp microelectrodes, and the information was acquired and analyzed with the pClamp8 program. Cellular and field spontaneous activity was exported from pClamp8 and analyzed with ad hoc programs written in MATLAB 7.0 (R14; MathWorks, Natick, MA). Samples of either 10 or 16 s were acquired every 20 s throughout the experiments (usually lasting >2 h), and they were digitalized at 400 Hz and notch filtered at 60 Hz. Windowed Fourier analysis was applied using a Hanning window with 50% overlap, and autocorrelograms of 2 s periods were also calculated. The levels of significance were calculated assuming a red noise background spectrum and a  $\chi^2$  distribution to find the 95% confidence contour (Torrence and Compo, 1998). Through a graphical user interface, we were able to simultaneously visualize spectrograms and to calculate specific peak values and mean values for spe-

cific user-defined frequency windows. To construct plots of the behavior of the frequency components throughout the different experimental conditions, the peak power was normalized with the mean peak power obtained from 15 samples recorded in control conditions. These data were then smoothed in time using a locally weighted least-squares second-degree fitting procedure resistant to outliers. Finally, the power versus time plots were standardized by interpolating and plotting a point/minute. Group plots are expressed as the mean  $\pm$  SEM.

**Drugs.** The drugs used were all prepared in the ACSF as follows: the NMDA receptor antagonist (DL)-2-amino-5-phosphonovaleric acid (APV) (30  $\mu\text{M}$ ; Tocris, Ballwin, MO); the non-NMDA receptor antagonist 6-nitro-7-sulfamoylbenzo (f) quinolaxine-2,3-dione (NBQX) (10  $\mu\text{M}$ ; Tocris); the  $\text{M}_1$ -acetylcholine-R antagonist pirenzepine (10  $\mu\text{M}$ ; Research Biochemicals, Natick, MA); the GABA<sub>A</sub> receptor antagonist bicuculline methiodide (20  $\mu\text{M}$ ; Sigma, St. Louis, MO); 4-aminopyridine (4-AP) (50  $\mu\text{M}$ ; Sigma); the group III metabotropic glutamate receptor (mGluR) agonist L-(+)-2-amino-4-phosphonobutyric acid (L-AP-4) (20  $\mu\text{M}$ ); the group II mGluR agonist (2S,2'R,3'R)-2-(2',3'-dicarboxycyclopropyl)glycine (DCG-IV) (1  $\mu\text{M}$ ); and the mGluR antagonist (+)-a-methyl-4-carboxyphenyl-glycine [(+)-MCPG] (500 mM; Tocris).

**Histological methods.** Slices containing biocytin-filled cells were fixed for 24 h in 4% paraformaldehyde (0.1 M phosphate buffer) and transferred to PBS containing 30% saccharose for 36 h. From these slices, 50- $\mu\text{m}$ -thick sections were obtained in a cryostat (Leica, Nussloch, Germany) that were collected in PBS, washed three times, and exposed to 0.3%  $\text{H}_2\text{O}_2$  for 30 min. After washing, the sections were processed free floating with the ABC kit (Vectastain; Vector Laboratories, Burlingame, CA) for 1 h in the presence of Triton X-100 (20  $\mu\text{l}/10$  ml). The slices were then rinsed three times in PBS, and the biotin-avidin complex was visualized with diaminobenzidine (10 mg/25 ml PBS at 10 mM; Sigma) for 10 min, contrasted for 10 min with nickel sulfate (30%). After rinsing several times, the slices were mounted in Entellan (Merck, Darmstadt, Germany)-treated slides, and cells were reconstructed with the aid of a drawing tube.

## Results

### Low-power spontaneous $\beta/\gamma$ activity in CA3

We conducted spectral fast Fourier transform (FFT) analysis on the spontaneous field activity recorded in the CA3 area of entorhinal cortex–hippocampal slices from control rats and from rats that had experienced either a single PTZ-induced seizure or 5–10 electrically kindled seizures. The *in vitro* recordings commenced 3–4 h after the PTZ or the electrical seizures were induced *in vivo*.

In our recording conditions, FFT analysis of the ongoing field activity recorded in normal ACSF from slices of PTZ-treated ( $n = 15$ ) and control ( $n = 15$ ) rats displayed strong frequency components below 8 Hz and clearly differentiated weaker spectral components between 20 and 24 Hz (Fig. 1*a,e*). Interestingly, in kindled rats that had experienced at least five seizures, the spectral components at frequencies below 8 Hz were much less prominent than in the animals in which a single seizure was induced. In contrast, the spectral component at  $19.9 \pm 0.2$  Hz ( $n > 20$ ), hereafter referred to as the “ $\sim 20$  Hz peak” (Fig. 1*b,e*), remained as a characteristic feature. Another characteristic spectral component of the kindled group was observed at  $181 \pm 0.6$  Hz ( $n = 10$ ; data not shown).

Because seizures induce cholinergic activity in CA3 (Gutiérrez and Heinemann, 2001; Romo-Parra et al., 2003), we tested the effect of the  $\text{M}_1$  cholinergic blocker pirenzepine on spontaneous activity. This antagonist depressed the  $\sim 20$  Hz peak in the animals exposed to PTZ (by  $23 \pm 0.3\%$ ) and in the kindled preparations (by  $27 \pm 1\%$ ), although it had only a mild effect on the 20–24 Hz band in control preparations ( $5 \pm 0.5\%$ ). Addition of the ionotropic GluR (iGluR) blockers NBQX (10  $\mu\text{M}$ ) and APV (30  $\mu\text{M}$ ) further diminished the power of all bands in the  $\beta/\gamma$

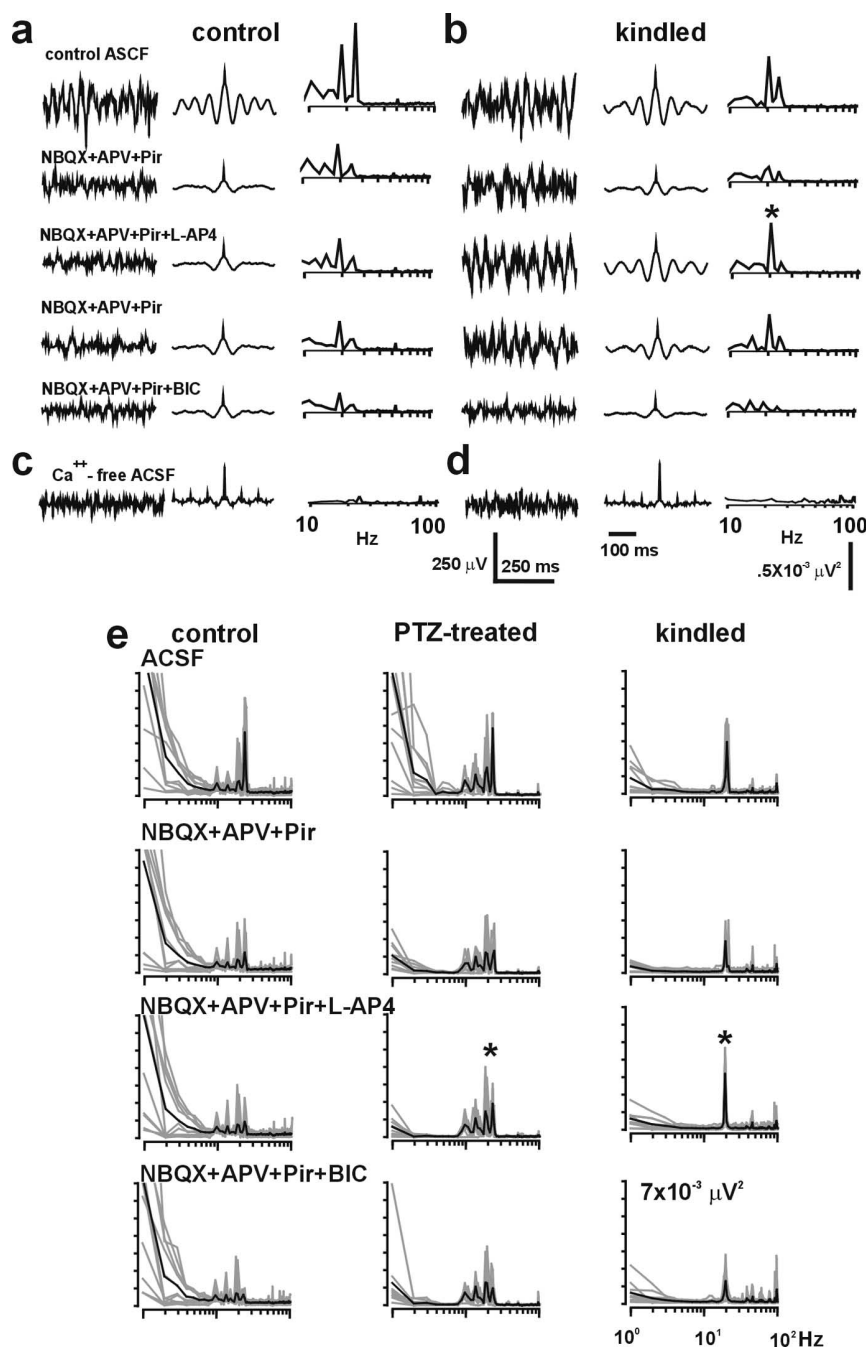


**Figure 1.** Spontaneous CA3 field activity from control and kindled preparations under different pharmacological conditions. Raw recordings from the CA3, and the corresponding autocorrelograms and spectrograms, taken from a preparation of a control rat (**a**) and a kindled rat (**b**). Components from 0 to 10 Hz were deleted from the spectrograms to enhance the resolution of the  $\beta/\gamma$  frequency band. After blockage of glutamatergic and cholinergic transmission (NBQX + APV + Pir), perfusion of L-AP-4 produced a significant and reversible potentiation of the GABA-mediated activity at  $\sim 20$  Hz in the kindled (asterisk) but not in the control preparation. Addition of bicuculline (BIC) depressed all components. **c, d**, Removing the  $\text{Ca}^{2+}$  from the ACSF fully depressed the ongoing activity and corresponding spectrograms. The peaks of the autocorrelograms in **a** and **b** are control at  $-43$  and  $+43$  ms ( $\sim 23$  Hz) and kindling at  $-49$  and  $+49$  ms ( $\sim 20$  Hz). **e**, Superimposed spectrograms of control, PTZ-treated, and kindled groups (gray lines;  $n = 10$ ), also showing the mean (black line), in the different pharmacological conditions. Asterisks indicate the L-AP-4-sensitive component in the PTZ-treated and kindled preparations.

frequency range, although the low-frequency components ( $< 10$  Hz) were more sensitive in the PTZ-treated and kindled groups than in the control rats (Fig. 1e). Adding bicuculline ( $20 \mu\text{M}$ ) further depressed all of the frequency components (Fig. 1a,b), in a similar manner to that observed when recordings were registered in a  $\text{Ca}^{2+}$ -

free solution (Fig. 1c,d). Thus, these responses suggest that spontaneous activity of the interneuron network underlies this component.

#### Activation of group III mGluR relieves the inhibition of GABA-mediated $\beta/\gamma$ activity in the CA3 after seizures

Activation of group III mGluR specifically inhibits the responses of the CA3 to DG activation mediated by GABA<sub>A</sub>R after seizures (Gutiérrez, 2000; Gutiérrez and Heinemann, 2001; Gutiérrez et al., 2003). Hence, we analyzed the effect of the agonist L-AP-4 ( $20 \mu\text{M}$ ) on the spontaneous field activity in the CA3 in slices of control rats and of rats subjected to one or several seizures. Specifically, we used an algorithm designed to determine the statistical significance of the changes of power in the whole spectrum or in user-defined frequency windows. In this manner, we assessed the effects of L-AP-4 on the spectrograms calculated from the spontaneous activity in the presence of NBQX plus APV plus pirenzepine. L-AP-4 did not produce changes in the GABA-mediated spontaneous activity of control rats (Fig. 1a,e). However, L-AP-4 did produce a significant and reversible potentiation of the spectral component at  $\sim 20$  Hz in PTZ-treated ( $68 \pm 10\%$ ;  $n = 12$ ;  $p < 0.05$ ) and kindled ( $305 \pm 8\%$ ;  $n = 10$ ;  $p < 0.05$ ) rats. In contrast, no changes were observed at other frequencies (Figs. 1b,e, 2a,b). We constructed a three-dimensional representation of the spectrograms obtained throughout an experiment on a kindled preparation under each of the pharmacological conditions (Fig. 2a). The effect of L-AP-4 on the normalized power of the  $\sim 20$  Hz peak in the control ( $n = 11$ ) and kindled ( $n = 10$ ) groups was also plotted (Fig. 2b). To enhance spontaneous activity and in an attempt to uncover other frequency bands modulated by activation of mGluR, the effect of L-AP-4 on the GABA-mediated spontaneous activity was also tested on control and PTZ-treated preparations in the presence of 4-AP at a concentration that did not produce epileptiform activity ( $50 \mu\text{M}$ ). Whereas perfusion of 4-AP enhanced the power of the  $\sim 20$  Hz peak by  $55 \pm 7\%$  and L-AP-4 produced an additional increment of  $27 \pm 12\%$  in rats that had experienced seizures ( $n = 12$ ; data not shown), these compounds were ineffective in control preparations. Finally, to uncover tonic activation of mGluR, the mGluR antagonist MCPG ( $500 \mu\text{M}$ ) was tested. This antagonist produced an inhibition of  $38 \pm 12\%$  ( $n = 6$ ) in the power of the GABA-mediated  $\sim 20$  Hz peak in kindled rats, although it had no effect in control rats (data not shown).

### The effect of mGluR activation on GABA-mediated $\beta/\gamma$ activity is prevented by disrupting the MF pathway

To determine whether the influence of L-AP-4 and MCPG on the GABA-mediated spontaneous activity of CA3 might be postsynaptic, we conducted the same type of experiments in slices 4 h after bisecting the MF pathway. Disrupting the MF pathway produced no major changes in the spectral components of control and PTZ-treated rats. In contrast, this manipulation consistently prevented the potentiating effect of L-AP-4 on the  $\sim 20$  Hz peak in PTZ-treated ( $n = 12$ ) and kindled ( $n = 12$ ) rats (Fig. 2*c,d*) and the inhibitory effect of MCPG in kindled rats ( $n = 6$ ; data not shown). The effect of L-AP-4 on the GABA-mediated spontaneous activity obtained in the presence of 4-AP was also impaired ( $n = 3$ ; data not shown).

### Activation of group III mGluR reverses inhibition, whereas activation of group II mGluR depresses spontaneous $\beta/\gamma$ activity in the CA3 after seizures

Because the results above were obtained in the presence of glutamatergic antagonists, we sought to determine the effect of L-AP-4 on spontaneous activity in normal ACSF. We also performed experiments with the group II mGluR agonist DCG-IV, because it is known to selectively depress glutamate release from the MF in the rat. Therefore, it was important to compare the effect of the agonists of both groups of mGluR to properly assess their presynaptic actions, especially because MF disruption was used to confirm the presynaptic action of L-AP-4 on field activity. The group III mGluR agonist L-AP-4 (20  $\mu\text{M}$ ) produced a significant increment in the power of the  $\sim 20$  Hz peak in PTZ-treated ( $70 \pm 7\%$ ;  $n = 19$ ) and kindled ( $84 \pm 11\%$ ;  $n = 3$ ) rats but not in control rats (Fig. 3*c,d*). In contrast to L-AP-4, the group II mGluR agonist DCG-IV (1  $\mu\text{M}$ ) produced a significant decrease in the power of virtually all spectral components in the  $\beta/\gamma$  range, with a marked inhibition ( $57 \pm 9\%$ ;  $n = 3$ ) of the  $\sim 20$  Hz peak in control rats (Fig. 3*a,b*). Interestingly, DCG-IV also effectively inhibited the  $\sim 20$  Hz peak in PTZ-treated ( $55 \pm 11\%$ ;  $n = 3$ ) and kindled ( $40 \pm 9\%$ ;  $n = 3$ ) rats (Fig. 3*c,d*). The specificity of the effects produced by both agonists was confirmed by performing the similar experiments 4 h after disrupting the MF pathway in a different set of slices. This manipulation prevented the effects of both mGluR agonists in control ( $n = 8$ ), PTZ-treated ( $n = 12$ ), and kindled ( $n = 6$ ) rats (Fig. 3*e,f*).

### L-AP-4 inhibits monosynaptic GABA<sub>A</sub>R-mediated responses presynaptically in pyramidal cells and SL interneurons after CA3 seizures

To explore the effects of L-AP-4 at the cellular level, we analyzed the synaptic responses evoked by DG stimulation in identified PyrC and SL-Int through intracellular recordings in slices from control, PTZ-treated, and kindled rats. In control rats, DG stim-

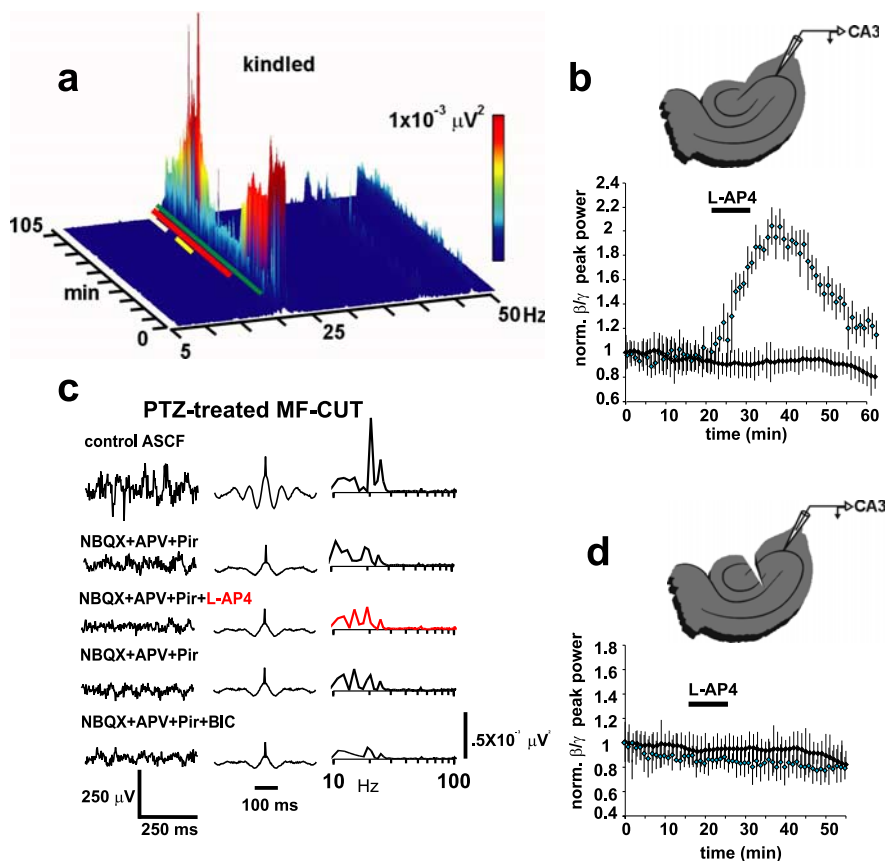


**Figure 2.** Potentiation of GABA-mediated  $\beta/\gamma$  activity through activation of mGluR III requires an intact DG-to-CA3 circuit. *a*, Three-dimensional layout of the spectrograms (from 5 to 50 Hz; *x*-axis) obtained throughout the experiment (*z*-axis), in the different pharmacological conditions. Spectral power is indicated in a color scale (*y*-axis) in which warm colors depict high power and cold colors depict low power. Colored lines over the mesh indicate the addition of pirenzepine (blue), NBQX plus APV (red), L-AP-4 (yellow), and bicuculline (white) to the normal ACSF. *b*, Effect of L-AP-4 on the GABA-mediated spontaneous oscillation at  $\sim 20$  Hz, expressed as the normalized power in control ( $n = 11$ ; black squares) and kindled ( $n = 10$ ; blue squares) groups. *c*, *d*, Disconnecting CA3 from the DG prevents the effect of L-AP-4 in the PTZ-treated and kindled groups ( $n = 7$ ).

ulation produced EPSP/IPSP sequences in both PyrC and SL-Int that were completely blocked by perfusion of NBQX and APV (Fig. 4*a,b*). However, whereas perfusion of NBQX plus APV plus pirenzepine blocked the EPSP in PTZ-treated and kindled rats, a short-latency IPSP could still be evoked in both cell types (Fig. 4*c,d*). The pharmacologically isolated IPSP had the same latency as the control EPSP ( $4.4 \pm 0.3$  ms for PyrC,  $n > 90$ ;  $4.8 \pm 0.6$  ms for SL-Int,  $n = 43$ ). Thus, the variability of the latency of the IPSP (and that of the EPSP) for each type of neuron is consistent with a monosynaptic contact (PyrC,  $F = 2.5$ ; SL-Int,  $F = 1.4$ ; one-way ANOVA test and Scheffé's post hoc ANOVA contrast,  $p < 0.01$ ) (Gutiérrez, 2002; Romo-Parra et al., 2003) (Fig. 4*a,b*). We then applied a paired-pulse stimulation protocol (interstimulus interval, 50 ms), which produced paired-pulse potentiation in both PyrC (IPSP<sub>2</sub>/IPSP<sub>1</sub>,  $1.2 \pm 0.1$ ;  $n = 17$ ) (Fig. 4*e*) and interneurons (IPSP<sub>2</sub>/IPSP<sub>1</sub>,  $1.2 \pm 0.3$ ;  $n = 4$ ) (Fig. 4*f*). Addition of L-AP-4 inhibited the first IPSP, producing an enhancement of the paired-pulse potentiation to  $3.6 \pm 0.2$  in PyrC and to  $2.2 \pm 0.2$  in SL-Int. This confirms that L-AP-4 acts presynaptically.

All interneurons identified electrophysiologically were recorded from the same region and presented IPSPs during MF activation in the presence of iGluR blockers. However, they were further characterized by performing an anatomical reconstruction of nine SL-Int (Fig. 5*a*) and nine PyrC (Fig. 5*b*) labeled with biocytin after recording. From the nine labeled SL-Int recorded at

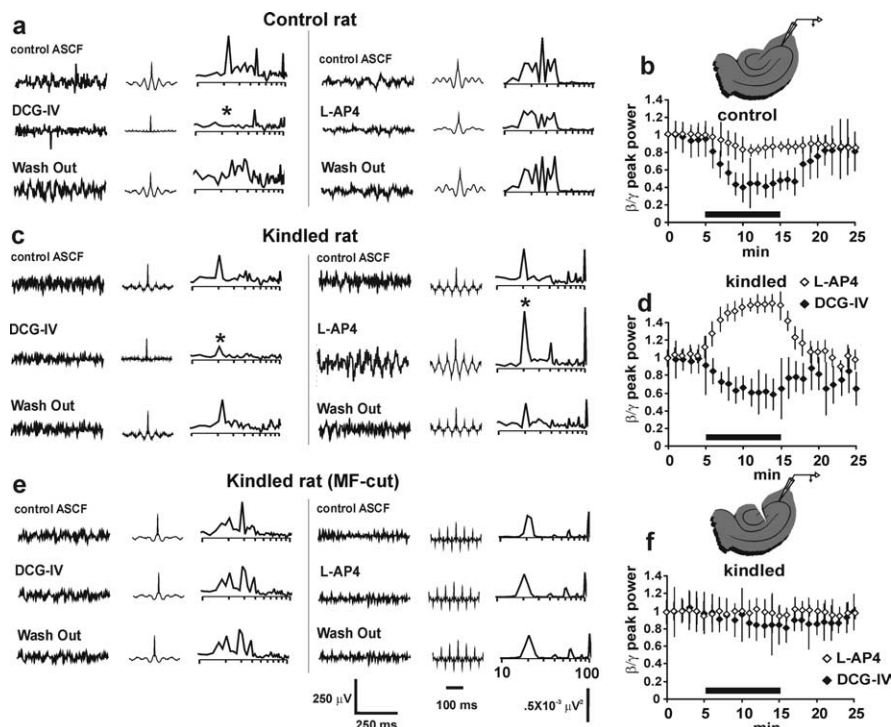


**Figure 3.** Activation of group III mGluR only potentiates  $\beta/\gamma$  activity after seizures, whereas activation of group II mGluR depresses this activity in control and kindled preparations. L-AP-4 potentiated the  $\sim 20$  Hz peak recorded in kindled ( $n = 3$ ; **a, b**) preparations but not in control ( $n = 3$ ; **a, b**) preparations. In contrast, DCG-IV inhibited this peak in both control ( $n = 3$ ; **a, b**) and kindled ( $n = 3$ ; **c, d**) preparations. **e, f**, Severing the MF prevented the effects of the agonists of both groups of mGluR ( $n = 8$  each group).

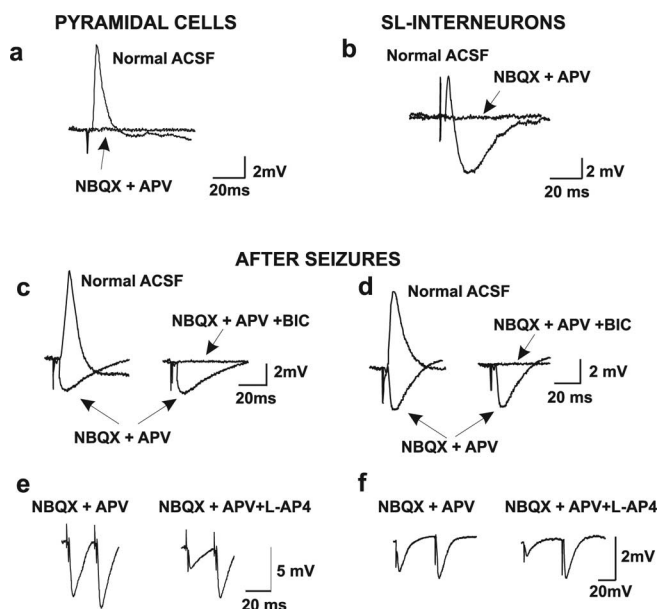


**Figure 4.** Emergence of MF-evoked GABA<sub>A</sub>-mediated monosynaptic responses in PyrC and SL-Int after seizures. In electrophysiologically and anatomically identified PyrC (**a**) and SL-Int (**b**) from control preparations, MF stimulation produced EPSP/IPSP sequences that were blocked by iGluR antagonists. **c, d**, In preparations from rats that were subjected to seizures, the same stimulation produced a monosynaptic GABA<sub>A</sub>-mediated IPSP in the presence of NBQX and APV. This IPSP was blocked by addition of bicuculline (BIC). A paired-pulse stimulation paradigm that produced potentiation of the second response was used to reveal the presynaptic inhibition of the GABA<sub>A</sub>-mediated responses by activation of mGluR III with L-AP-4. The first response to the pair of pulses was depressed by L-AP-4, whereas the IPSP<sub>2</sub>/IPSP<sub>1</sub> ratio was enhanced, in both pyramidal cells (**e**) and interneurons (**f**). The anatomical reconstruction of the recorded cells is depicted in Figure 5.

the border between strata pyramidale and lucidum of the CA3, six had the typical features of basket cells (Fig. 5*a*), whereas three were bistratified cells (data not shown).

#### L-AP-4 potentiates spontaneous subthreshold membrane $\beta/\gamma$ oscillations mediated by GABA in pyramidal cells and SL interneurons after seizures

Because the spiking frequency of cells in the slice is very low or spikes are absent in the presence of iGluR blockers, we analyzed the spontaneous subthreshold membrane  $\beta/\gamma$  oscillations (SSMO) of PyrC and SL-Int. We recorded the intracellular spontaneous activity, and we performed FFT and wavelet analysis from 10 s samples acquired every 30 s throughout the experiments. A spectral analysis was performed on a random sample of 10 PyrC and 10 SL-Int from each experimental group in the different pharmacological conditions (Fig. 6). Low-frequency activity (below 10 Hz) was the predominant spectral component in both the PyrC and SL-Int. During perfusion of iGluR and ACh receptor antagonists, the SSMO spectrograms of the SL-Int from control preparations presented a weak  $\sim 20$  Hz

peak (Fig. 6*a*), although this peak was virtually absent in PyrC (Fig. 6*a*). This  $\sim 20$  Hz component was barely detectable in PyrC from PTZ-treated preparations (Fig. 6*b*), although it was significantly enhanced in kindled preparations that had suffered at least five seizures ( $104 \pm 11\%$  enhancement;  $p = 0.001$ ;  $n = 10$ ) (Fig. 6*c*). Perfusion of L-AP-4 produced a potentiation of  $15 \pm 6\%$  of the  $\sim 20$  Hz peak in PyrC of PTZ-treated rats ( $p = 0.39$ ;  $n = 10$ ) (Fig. 6*b*) and an enhancement of  $27 \pm 10\%$  in those of kindled rats ( $p = 0.003$ ;  $n = 10$ ) (Fig. 6*c*). In contrast to PyrC, the SSMO of control and PTZ-treated SL-Int presented a notable  $\sim 20$  Hz peak on perfusion of glutamatergic antagonists, which was reversibly potentiated by L-AP-4 ( $161 \pm 7\%$ ;  $p = 0.0001$ ;  $n = 10$ ) (Fig. 6*b*).

The proportion of cells that presented SSMO with frequency components matching those observed in the spectrograms of field recordings was determined in the PyrC and SL-Int of control and PTZ-treated preparations and in the PyrC from kindled preparations under all pharmacological conditions. Accordingly, all PyrC have components at the  $\theta$  and  $\beta$  frequencies, and a small percentage displays SSMO at  $\gamma$  frequencies. Interestingly, L-AP-4 not only produced a potentiation of  $\beta$  activity in kindled rats, but this activity was also observed in more PyrC (Fig. 6). In contrast, in control and PTZ-treated preparations, the percentage of PyrC displaying  $\beta$  activity was not significantly modified. Conversely, the proportion of SL-Int cells that presented spectral components at  $\beta$  and  $\gamma$  frequencies significantly increased in PTZ-treated preparations when compared with control preparations (no SL-Int were recorded from kindled preparations). Unlike PyrC, L-AP-4 further increased the proportion of SL-Int involved in the  $\beta$  and  $\gamma$  activity in these animals (Fig. 6*d*), reminiscent of the behavior of the spontaneous field oscillations.

### Activation of the MF at $\theta$ , $\beta$ , and $\gamma$ frequencies restrains pyramidal cells, although it entrains SL-interneurons to induce spiking activity in a frequency-dependent manner

We explored the differences in the integration of dual glutamatergic–GABAergic signaling from the MF in PyrC and SL-Int. As such, synaptic responses were evoked by repetitive activation of the MF in normal ACSF, at frequencies characteristic of the spectrograms of the spontaneous field and cellular activity. Pulses of 0.1 ms were delivered to the DG at a current intensity that evoked 60% of the EPSP amplitude needed to reach the threshold to evoke action potentials, at 10 ( $\theta$ ) and 20 ( $\beta$ ) during 2 s as well as at 50 Hz ( $\gamma$ ) for 1 s. The resting membrane potential of PyrC from control and post-seizure animals did not display significant differences (control,  $-63 \pm 2$  mV,  $n = 60$ ; PTZ-treated,  $-63 \pm 1$  mV,  $n = 50$ ; kindling,  $-64 \pm 1$  mV,  $n = 60$ ). However, more hyperpolarized values were registered in the SL-Int from PTZ-treated preparations ( $-68 \pm 1$  mV;  $n = 65$ ) than from control preparations ( $-63 \pm 4$  mV;  $n = 15$ ). We calculated the number of spikes generated during the train of stimuli. The activation of the DG produces a summation of EPSPs in a frequency-dependent manner that reached the threshold to evoke action potentials more effectively in control PyrC when compared with the PyrC of PTZ-treated (post-seizure) preparations (Fig. 7, compare  $a_1, b_1, c_1$  with  $a_2, b_2, c_2$ ). A restraining effect could be observed on the number of action potentials generated during the trains in PTZ-treated preparations at 10 and 20 Hz (Fig. 7*a*<sub>3</sub>, *b*<sub>3</sub>). As such, the PTZ-treated PyrC fired 28% less at 10 Hz and 53% less at 20 Hz ( $n = 6$ ) than control PyrC cells. At 50 Hz, the number of action potentials generated during the first 20 stimuli of the train was similar in both preparations, but, after 50 stimuli, this number was higher in PTZ-treated rats (data not shown). In contrast, stimulation of the DG was more effective in producing summation of EPSPs to generate action potentials in the SL-Int of PTZ-treated preparations (Fig. 7*d*<sub>2</sub>) when compared with control ones (Fig. 7*d*<sub>1</sub>). These results show that, despite the emergence of MF GABAergic transmission, activation of the MF readily entrains the SL-Int to generate action potentials. In turn, the PyrC are strongly inhibited by this forward mechanism, which can be directly potentiated by MF GABAergic transmission (Treviño and Gutiérrez, 2005).

### Discussion

Two  $\beta/\gamma$  generators have been proposed to reside in the hippocampus: an oscillator in the DG that is driven from an extrahippocampal source, and a generator in the CA3 that does not require external

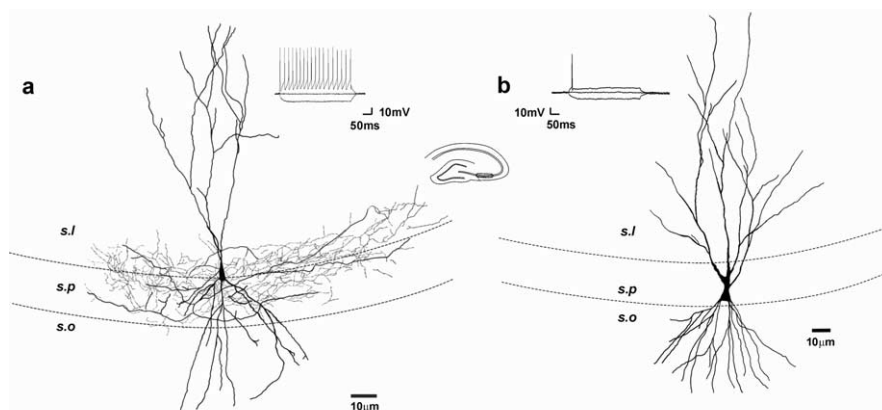


**Figure 5.** Camera lucida reconstructions of an intracellular labeled basket cell at the border between the strata pyramidale and lucidum (*a*) and of a pyramidal cell (*b*). The firing behavior in response to a transmembrane depolarizing current (insets) was in agreement with the anatomical characterization. The synaptic responses of the depicted cells are presented in Figure 4. s.l., Stratum lucidum; s.p., stratum pyramidale; s.o., stratum oriens.

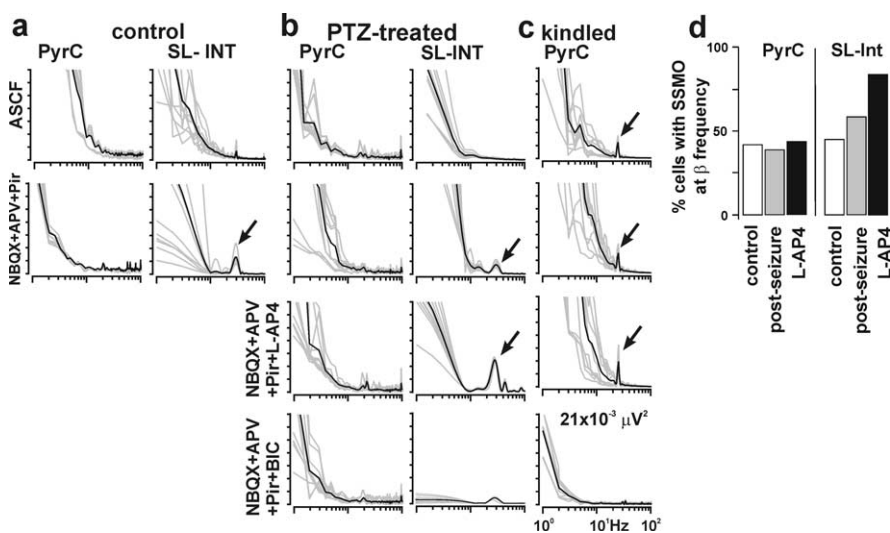


**Figure 6.** Spectrograms of subthreshold membrane oscillations SSMOs of PyrC and SL-Int recorded intracellularly ( $n = 10$  per panel plus mean; black line) in hippocampal slices of control (*a*), PTZ-treated (*b*), and kindled (*c*) rats under different pharmacological conditions. *a*, Control cells. *b*, As in the field recordings, L-AP-4 produced a significant potentiation of the  $\sim 20$  Hz peak (asterisk) in the SSMO SL-Int of the PTZ-treated group, whereas a milder effect was observed in those of PyrC. *c*, In kindled preparations, the effect of L-AP-4 on SSMOs was also noticeable in PyrC. *d*, Proportion of pyramidal cells and interneurons displaying SSMO at 20–24 Hz from control and PTZ-treated rats. SSMO of PyrC [control,  $n = 18$ ; PTZ-treated (post-seizure),  $n = 18$ ] and of SL-Int [control,  $n = 6$ ; PTZ-treated (post-seizure),  $n = 12$ ] were recorded in the presence of iGluR blockers and iGluR blockers plus L-AP-4. Notice that the proportion of SL-Int displaying SSMO at the  $\beta$  frequency band slightly increased after seizures and was significantly enhanced in the presence of L-AP-4, whereas the proportion of PyrC remained unaffected.

inputs. In this paper, we show that, in hippocampal slices from rats that have suffered seizures, the  $\beta/\gamma$  oscillations in the CA3 area are tonically modulated by aberrant GABA-mediated neurotransmission from the DG. Moreover, this modulation is exerted on GABA oscillations in the interneuronal network, as confirmed in the presence of GABA<sub>A</sub>R antagonists. This modulation appears after seizures, and it acts in the inhibitory direction because of the following: (1) the MF–GABAergic input produces GABA<sub>A</sub>R-mediated monosynaptic IPSPs in PyrC and SL-Int; (2) the CA3 area is neither excited nor its normal feedforward inhibition reversed by aberrant GABAergic input (Treviño and Gutiérrez, 2005); and (3) activation of mGluR potentiates spontaneous network oscillations, despite selectively inhibiting GABA release from the MF (Fig. 8).

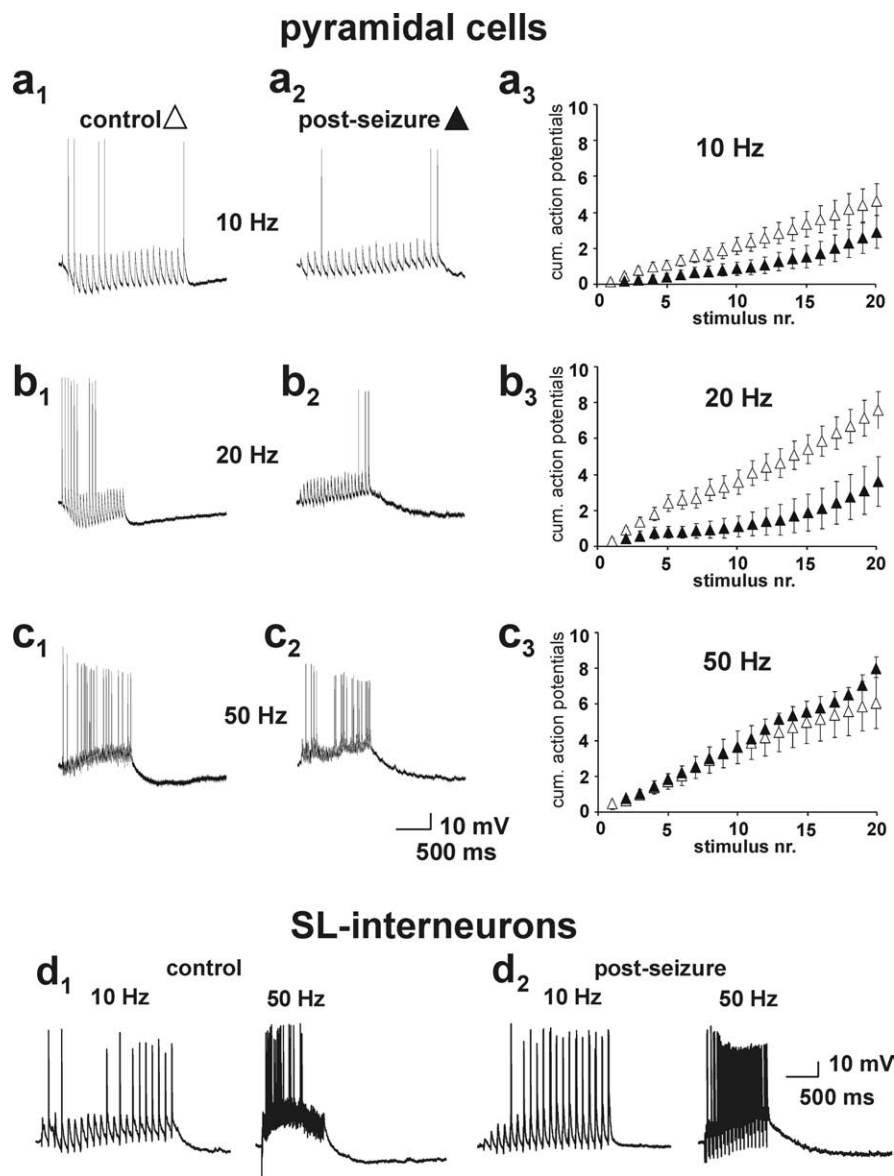


**Figure 7.** Intracellular responses of PyrC and SL-Int to high-frequency stimulation of the MF. Responses of control PyrC (**a<sub>1</sub>–c<sub>1</sub>**) and post-seizure PyrC (**a<sub>2</sub>–c<sub>2</sub>**) to increasing stimulation frequencies. **c<sub>1</sub>–c<sub>3</sub>**, Corresponding plots of cumulative action potentials along the trains of the control ( $n = 6$ ) and post-seizure ( $n = 10$ ) groups. Note that MF stimulation is less effective in eliciting action potentials in post-seizure than control PyrC. Moreover, inhibition of PyrC spiking is more pronounced at 20 Hz, consistent with a resonance phenomenon. **d**, In contrast to its effects on PyrC, high-frequency MF stimulation shows higher efficacy in producing action potentials in SL-Int of post-seizure than in control preparations.

Recurrent excitation between pyramidal neurons has been viewed as an important means source to generate rhythms and to synchronize neurons. However, because recurrent connections between PyrC alone cannot account for the network coherence during oscillations, PyrC populations may be entrained by synchronous rhythmic inhibition originating from interneurons (Wang and Buzsáki, 1996). Indeed, interneuron-mediated  $\gamma$  activity may be active in the absence of glutamatergic transmission and it might be driven by activation of mGluR, whereby the timing of the oscillations varies depending on GABAergic transmission (Traub et al., 1996). Our data show that MF inputs might also be involved in modulating interneuron-mediated  $\beta/\gamma$  oscillations in the CA3 by acting on GABA receptors, primarily on those located in their major targets, the SL-Int. Our evidence suggests that, in contrast to the GABAergic input from the inter-

neurons, GABAergic input from the MF disorganizes the periodic interneuron inhibition, because oscillations increase when the MF GABA output is depressed with L-AP-4 (Fig. 8).

Because the MF are functionally compartmentalized (Maccaferri et al., 1998), it is reasonable to consider the possibility that the characteristics of the release of GABA from the MF could also depend on the type of target onto which they impinge. We show here that, although the simultaneous glutamatergic and GABAergic transmission from the MF is expressed onto both PyrC and SL-Int, activation of this pathway does not release the normal feedforward inhibition in the CA3 area (Treviño and Gutiérrez, 2005). This is attributable to the fact that MF glutamatergic transmission readily entrains SL-Int into spiking activity and this, in turn, restrains PyrC spiking in a frequency-dependent manner. Indeed, granule cells entrain their target cells in an activity-dependent manner (Henze et al., 2002). Each granule cell innervates 40–50 interneurons and 11–18 PyrC (Amaral et al., 1990; Acsády et al., 1998), and granule cells are very effective at recruiting interneurons. Thus, these cells serve to amplify and sustain the GABAergic modulation of the CA3.

The power gain observed at the  $\beta/\gamma$  frequency during activation of group III mGluR in animals that experienced seizures could reflect a relaxation of GABAergic inhibitory control of CA3 SL-Int through a decrease in the GABA output from the MF. Indeed, we have shown that this effect is prevented by bisecting the MF pathway, thereby excluding the postsynaptic activity of L-AP-4 (Fig. 8). We show that this effect was more evident after several kindled seizures. This, together with the appearance of very high-frequency oscillations probably reflect long-lasting changes and remodeling of the MF–CA3 network (Behrens et al., 2005).

We rarely observed spontaneous spiking activity of the PyrC and SL-Int, especially in the presence of iGluR antagonists. However, spectral analysis of the spontaneous field activity showed that, although low frequencies were dominant in the spectrograms ( $< 8$  Hz), a spectral peak in the  $\beta/\gamma$  band between 20 and 24 Hz could clearly be differentiated after expanding the resolution of the spectrograms. This spectral peak was also present in the SSMO of PyrC and interneurons, as reported previously (Fischer, 2004). Interestingly, the activation of group III mGluR potentiated not only the spectral peak observed in field recordings but also the SSMO displayed by SL-Int. Furthermore, this effect was also observed in the SSMO of PyrC in kindled animals. A high-power oscillation at 20 Hz in the CA3 can be induced by cholinergic agonists (Mann et al., 2005b), an effect that we observed by activating group III mGluR. The mGluR-sensitive MF–GABAergic input may be an effective

means to regulate oscillatory activity in both the PyrC and SL-Int. Thus, our data are in line with the proposal that the DG plays a passive role in the generation of oscillations and that it is not essential for intrinsically generated oscillations (Fischer, 2004). However, the DG does seem to play an active role in modulating  $\beta/\gamma$  oscillations after seizures through GABAergic activity. Moreover, we observed resonance during stimulation of the DG at the frequency at which the CA3 oscillates. Indeed, in post-seizure preparations, the stimulation of the MF at a frequency that matches the CA3 oscillations results in the maximal restriction of the generation of action potentials in PyrC. This probably serves to maximize forward inhibition, and it may be reinforced by monosynaptic GABAergic inhibition exerted by the MF.

Experimental *in vitro*  $\beta/\gamma$  oscillations occur in conditions in which both PyrC and SL-Int are influenced by mGluR and cholinergic receptors (Traub et al., 1998). Agonists of group I mGluR induce persistent  $\beta/\gamma$  oscillations that appear to require the loss of excitation in interneurons (Traub et al., 2005). We show here that this activity driven by GABA develops in rats that experienced a single seizure and is augmented in kindled rats. Moreover, this activity can be potentiated by activation of group III mGluR attributable to the suppression of the inhibitory tone of the MF. In contrast, blocking mGluR with MCPG depresses  $\beta/\gamma$  field activity in epileptic but not in control rats. Interestingly, severing the MF also impedes this modulation. We proposed previously that L-AP-4 selectively modulates GABA release from the MF, whereas DCG-IV primarily inhibits glutamate release (Gutiérrez, 2002). Accordingly, we show that L-AP-4 depresses the release of GABA from the MF while the inhibition of  $\beta/\gamma$  field activity is released, whereas DCG-IV strongly depresses  $\beta/\gamma$  field activity and MF neurotransmission. Because severing the MF pathway prevents these effects, both groups of mGluR would appear to be present in MF axons and terminals (Shigemoto et al., 1997).

### Functional implications

Generalized seizures are followed by a period of depression (postictal depression), during and after which memory and cognitive deficits develop. Thus, activity-dependent tonic inhibition of the CA3 region of the hippocampus via the DG, and particularly of its oscillatory activity, constitutes a mechanism that may underlie these deficits. Indeed, not only is information transfer from the DG to the CA3 region more complex after the establishment of epilepsy (Gutiérrez and Heinemann, 2001) by means of a (window) filtering mechanism (Heinemann et al., 1992; present data) but, as we now show, the DG also tonically modifies the ongoing activity in the CA3.

Recent results suggest that the CA3 region is hypoactive after epileptic seizures (Biagini et al., 2005), and this possibility can be also supported by our data showing that the MF–GABAergic input both directly inhibits PyrC (Gutiérrez, 2000; Gutiérrez and

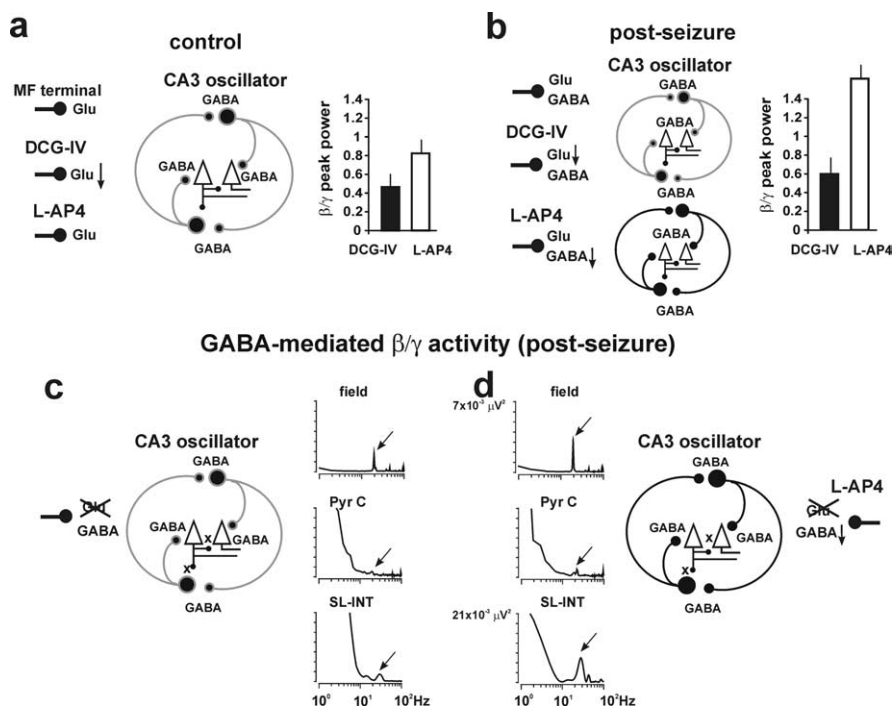


**Figure 8.**  $\beta/\gamma$  activity in the CA3 region is inhibited by mGluR-sensitive, GABA-mediated aberrant transmission from the MF. **a**, CA3 is an endogenous oscillator that receives a glutamatergic input from the MF. Activation of group II mGlu presynaptic receptors inhibits glutamate release from the MF and strongly depresses oscillatory activity, whereas activation of group III mGluR produces a modest inhibition. In rats subjected to seizures **b**, the activation of group III mGlu presynaptic receptors with L-AP-4, which inhibits GABA release from the MF, produces a noticeable enhancement of the  $\beta/\gamma$  power. This uncovers the tonic inhibitory control of the MF on the oscillatory activity. This control is exerted on GABA-mediated oscillations because it is observed in the presence of iGluR blockers. **c**, Indeed, in the absence of glutamatergic input, GABA-mediated oscillatory  $\beta/\gamma$  activity (arrows) can be observed in field recordings and in SSMO of SL-Int of area CA3 after seizures. **d**, Activation of group III mGluR relieves the inhibition of GABA-mediated  $\beta/\gamma$  oscillations (arrows) in the CA3 field, which is primarily reflected in the SSMO of SL-Int.

Heinemann, 2001; Romo-Parra et al., 2003) and produces presynaptic inhibition of collateral MF (Ruiz et al., 2003; Treviño and Gutiérrez, 2005). Thus, this increased inhibition can probably protect against the additional generation of seizures.

Besides temporally linking neurons into assemblies, network oscillations introduce a bias on input selection and facilitate synaptic plasticity. These mechanisms cooperate to support temporal representation and long-term consolidation of information (Buzsáki and Draguhn, 2004), and, thus, oscillations can boost or hamper epileptogenic events (Traub et al., 2004). It has been acknowledged that the MF input regulates the subthreshold activation of voltage-gated ion channels in CA3 PyrC by dynamically regulating their sensitivity to inputs. As such, the strength of a given input or the likelihood that an input is potentiated will depend on the time of its arrival with respect to the most recent MF input (Urban and Barrionuevo, 1998). Additionally, MF GABA release could introduce a modulatory factor reflected in the variance of inhibitory activity, which in turn could strongly modulate the efficacy of GABAergic inhibition and glutamatergic excitation (Aradi and Soltesz, 2002; Aradi et al., 2002).

In summary, our results show that the emergence of aberrant MF GABAergic transmission is a physiologically relevant signal that modulates the spontaneous activity of the CA3, probably regulating the flow of information from the entorhinal cortex to the hippocampus itself after seizures. Moreover, we propose that both interneurons and the principal cells of the DG may be engaged in setting the tone for oscillations to be expressed or suppressed in the hippocampus.

## References

- Acsády L, Kamondi A, Sik A, Freund T, Buzsáki G (1998) GABAergic cells are the major postsynaptic targets of mossy fibers in the hippocampus. *J Neurosci* 18:3386–3403.
- Amaral DG, Ishizuka N, Claiborne B (1990) Neurons, numbers and the hippocampal network. *Prog Brain Res* 83:1–11.
- Aradi I, Soltesz I (2002) Modulation of network behaviour by changes in variance in interneuronal properties. *J Physiol (Lond)* 538:227–251.
- Aradi I, Santhakumar V, Chen K, Soltesz I (2002) Postsynaptic effects of GABAergic synaptic diversity: regulation of neuronal excitability by changes in IPSC variance. *Neuropharmacology* 43:511–522.
- Behrens CJ, van den Boom LP, de Hoz L, Friedman A, Heinemann U (2005) Induction of sharp wave–ripple complexes in vitro and reorganization of hippocampal networks. *Nat Neurosci* 8:1560–1567.
- Biagini G, D’Arcangelo G, Baldelli E, D’Antuono M, Tancredi V, Avoli M (2005) Impaired activation of CA3 pyramidal neurons in the epileptic hippocampus. *Neuromolecular Med* 7:325–342.
- Bragin A, Jando G, Nadasdy Z, Hetke J, Wise K, Buzsáki G (1995) Gamma (40–100 Hz) oscillation in the hippocampus of the behaving rat. *J Neurosci* 15:47–60.
- Buzsáki G, Chrobak JJ (1995) Temporal structure in spatially organized neuronal ensembles: a role for interneuronal networks. *Curr Opin Neurobiol* 5:504–510.
- Buzsáki G, Draguhn A (2004) Neuronal oscillations in cortical networks. *Science* 304:1926–1929.
- Csicsvari J, Jamieson B, Wise KD, Buzsáki G (2003) Mechanisms of gamma oscillations in the hippocampus of the behaving rat. *Neuron* 37:311–322.
- Fischer Y (2004) The hippocampal intrinsic network oscillator. *J Physiol (Lond)* 554:156–174.
- Gómez-Lira G, Lamas M, Romo-Parra H, Gutiérrez R (2005) Programmed and induced phenotype of the hippocampal granule cells. *J Neurosci* 25:6939–6946.
- Gutiérrez R (2000) Seizures induce simultaneous GABAergic and glutamatergic neurotransmission in the dentate gyrus-CA3 system. *J Neurophysiol* 84:3088–3090.
- Gutiérrez R (2002) Activity-dependent expression of simultaneous glutamatergic and GABAergic neurotransmission from the mossy fibers in vitro. *J Neurophysiol* 87:2562–2570.
- Gutiérrez R (2005) The dual glutamatergic-GABAergic phenotype of the hippocampal granule cells. *Trends Neurosci* 28:297–303.
- Gutiérrez R, Heinemann U (2001) Kindling induces transient fast inhibition in the dentate gyrus-CA3 projection. *Eur J Neurosci* 13:1371–1379.
- Gutiérrez R, Romo-Parra H, Maqueda J, Vivar C, Ramírez M, Morales MA, Lamas M (2003) Plasticity of the GABAergic phenotype of the “glutamatergic” granule cells of the rat dentate gyrus. *J Neurosci* 23:5594–5598.
- Heinemann U, Beck H, Dreier JP, Ficker E, Stabel J, Zhang CL (1992) The dentate gyrus as a regulated gate for the propagation of epileptiform activity. In: *The dentate gyrus and its role in seizures (Epilepsy Research Supplement 7)* (Ribak CE, Gall CM, Mody I, ed), pp 273–280. Amsterdam: Elsevier.
- Henze DA, Wittner L, Buzsáki G (2002) Single granule cells reliably discharge targets in the hippocampal CA3 network in vivo. *Nat Neurosci* 5:790–795.
- Kasyanov AM, Safulina VF, Voronin LL, Cherubini E (2004) GABA-mediated giant depolarizing potentials as coincidence detectors for enhancing synaptic efficacy in the developing hippocampus. *Proc Natl Acad Sci USA* 101:3967–3972.
- Maccaferri G, Tóth K, McBain CJ (1998) Target-specific expression of presynaptic mossy fiber plasticity. *Science* 279:1368–1370.
- Mann EO, Radcliffe CA, Paulsen O (2005a) Hippocampal gamma-frequency oscillations: from interneurons to pyramidal cells, and back. *J Physiol (Lond)* 562:55–63.
- Mann EO, Suckling JM, Hájos N, Greenfield SA, Paulsen O (2005b) Perisomatic feedback inhibition underlies cholinergically induced fast network oscillations in the rat hippocampus in vitro. *Neuron* 45:105–117.
- Romo-Parra R, Vivar C, Maqueda J, Morales MA, Gutiérrez R (2003) Activity-dependent induction of multitransmitter signaling onto pyramidal cells and interneurons of area CA3 of the rat hippocampus. *J Neurophysiol* 89:3155–3167.
- Ruiz A, Fabian-Fine R, Scott R, Walker MC, Rusakov DA, Kullmann DM (2003) GABA<sub>A</sub> receptors at hippocampal mossy fibres. *Neuron* 39:961–973.
- Safulina VF, Fattorini G, Conti F, Cherubini E (2006) GABAergic signaling at mossy fiber synapses in neonatal rat hippocampus. *J Neurosci* 26:597–608.
- Sejnowski TJ, Paulsen O (2006) Network oscillations: emerging computational principles. *J Neurosci* 26:1673–1676.
- Shigemoto R, Kinoshita A, Wada E, Nomura S, Ohishi H, Takada M, Flor PJ, Neki A, Abe T, Nakanishi S, Mizuno N (1997) Differential presynaptic localization of metabotropic glutamate receptor subtypes in the rat hippocampus. *J Neurosci* 17:7503–7522.
- Torrence C, Compo GP (1998) A practical guide to wavelet analysis. *Bull Am Meteor Soc* 79:61–78.
- Treviño M, Gutiérrez R (2005) The GABAergic projection of the dentate gyrus to hippocampal area CA3 of the rat: pre- and postsynaptic actions after seizures. *J Physiol (Lond)* 567:939–949.
- Traub RD, Whittington MA, Colling SB, Buzsáki G, Jefferys JGR (1996) Analysis of gamma rhythms in the rat hippocampus in vitro and in vivo. *J Physiol (Lond)* 493:471–484.
- Traub RD, Spruston N, Soltesz I, Konnerth A, Whittington MA, Jefferys JGR (1998) Gamma-frequency oscillations: a neuronal population phenomenon, regulated by synaptic and intrinsic cellular processes, and inducing synaptic plasticity. *Prog Neurobiol* 55:563–575.
- Traub RD, Bibbig A, LeBeau FEN, Buhl EH, Whittington MA (2004) Cellular mechanisms of neuronal population oscillations in the hippocampus in vitro. *Annu Rev Neurosci* 27:247–278.
- Traub RD, Pais I, Bibbig A, LeBeau FEN, Buhl EH, Garner H, Monyer H, Whittington MA (2005) Transient depression of excitatory synapses on interneurons contributes to epileptiform bursts during gamma oscillations in the mouse hippocampal slice. *J Neurophysiol* 94:1225–1235.
- Urban NN, Barrionuevo G (1998) Active summation of excitatory postsynaptic potentials in hippocampal CA3 pyramidal neurons. *Proc Natl Acad Sci USA* 95:11450–11455.
- Walker MC, Ruiz A, Kullmann DM (2001) Monosynaptic GABAergic signaling from dentate to CA3 with a pharmacological and physiological profile typical of mossy fibre synapses. *Neuron* 29:703–715.
- Wang XJ, Buzsáki G (1996) Gamma oscillation by synaptic inhibition in a hippocampal interneuronal network model. *J Neurosci* 16:6402–6413.